C h a p t e r 3

COUPLED CONSOLIDATION

3.1. INTRODUCTION

In soil mechanics, the term consolidation describes the volumetric deformations of soil that occur due to changes in effective stress. The rate at which consolidation occurs in saturated soil is determined by the rate at which the pore fluid can flow out of the soil. Hence, the processes of deformation and pore fluid flow in soil are coupled. The review of deep excavation literature in Chapter 2 showed the importance of consolidation for deep excavations in clay. Consolidation is also important in many other geotechnical problems such as foundations, tunnels, and embankments. It is therefore often important to include coupled consolidation finite element analyses of geotechnical problems.

The two dimensional finite element program, SAGE, created at Virginia Tech for analyzing static soil-structure interaction, did not include coupled consolidation (Morrison, 1995). Therefore, coupled consolidation was implemented into SAGE in the course of this research study in order to expand its capabilities and usefulness. The finite element formulation of coupled consolidation, the computer implementation of coupled consolidation into SAGE, and the results of three verification problems are presented in this chapter.

3.2. FINITE ELEMENT FORMULATION

Biot (1940) was the first to publish a derivation of coupled consolidation and an analytical solution. Biot used the following assumptions in his derivation of coupled consolidation.

1. The soil is a two-phase continuum made up of solid soil particles and a fluid.
2. The fluid is incompressible, and the soil is saturated.
3. The soil particles are incompressible, but the soil skeleton (the assemblage of soil particles) is compressible.
4. Darcy's Law governs the flow of the fluid through the soil.
5. Small strain theory applies.

Although the first assumption is not true on the scale of individual particles, it is a good approximation for engineering purposes since the size of the soil particles and pore fluid molecules are much smaller than the dimensions of practical interest, and it simplifies the mathematical treatment of the problem. The second assumption is reasonable since the pore fluid in soils is typically water, which is essentially incompressible relative to the soil skeleton. The third assumption is reasonable since the volume change of the soil skeleton is much larger than the volume change of the soil particles.

The equations of equilibrium provide the first set of governing equations for coupled consolidation:

$$\sigma_{ij,j} = 0 \qquad \text{Equation 3.1}$$

Where i and j are indices from 1 to 3 and represent directions in a Cartesian coordinate system (x_1, x_2, x_3). σ_{ij} is the total stress tensor at a material point (x_1, x_2, x_3) in the soil. The notation "$,j$" represents a partial derivative with respect the x_j direction ($\delta/\delta x_j$). Therefore, Equation 3.1 represents three independent equations (i.e. equilibrium of forces in the x_1, x_2, and x_3 directions).

The principle of effective stress says that the total stress, σ, is equal to the sum of the effective stress, σ', and hydrostatic pressure, p_w, in the pore fluid. When the principle of effective stress is incorporation, Equation 3.1 becomes:

$$\sigma_{ij,j} = \sigma'_{ij,j} + p_{w,j} = 0 \qquad \text{Equation 3.2}$$

The second governing equation of the coupled consolidation problem is the transient seepage equation:

$$v_{i,i} - \dot{\varepsilon}_{ii} = 0 \qquad \text{Equation 3.3}$$

Where $v_{i,i}$ is the gradient of the velocity of the pore fluid and $\dot{\varepsilon}_{ii}$ is the volumetric strain rate. Equation 3.3 means that the net flow rate of the pore fluid out of a volume of saturated soil is equal to the rate at which the volume of saturated soil is decreasing. v_i is assumed to be governed by Darcy's Law:

$$v_i = k_{ij} h_{,j} \qquad \text{Equation 3.4}$$

Where k_{ij} is the permeability matrix and $h_{,j}$ is the total head gradient in the x_j direction. The total pore water head, h, is a measure of the potential energy of the pore fluid and is given by:

$$h = (x_2 - x_{2_{DATUM}}) + \frac{p_w}{\gamma_w} \qquad \text{Equation 3.5}$$

Where x_2 is the direction in which gravity acts and $x_{2_{DATUM}}$ represents a plane to which the total head is referenced.

Equations 3.2, 3.3, and 3.4 are the governing equations for coupled consolidation of soils. The derivation for the finite element formulation of the coupled consolidation problem from Equations 3.2, 3.3, and 3.4 is given in Appendix A. The finite element formulation derived in Appendix A is:

$$\begin{bmatrix} [K] & [K_v]^T \\ [K_v] & \Delta t\theta[K_h] \end{bmatrix} \begin{Bmatrix} \{\Delta d\} \\ \{\gamma_w h\}\big|_{t+\Delta t} \end{Bmatrix} = \begin{Bmatrix} \{F\}\big|_{t+\Delta t} - \{F\}\big|_t + [K_v]^T\{\gamma_w h\}\big|_t \\ \Delta t\left(\{Q\}\big|_{t+\Delta t} - \{Q\}\big|_t\right) - \Delta t(1-\theta)[K_h]\{\gamma_w h\}\big|_t \end{Bmatrix}$$

Equation 3.6

Where,

$\left[K\right]$	is the stiffness matrix; $\left[K\right]=\int_{\Omega}\left[B\right]^{T}\left[D\right]\left[B\right]d\Omega$.
$\left[K_v\right]$	is the coupling matrix; $\left[K_v\right]=\int_{\Omega}\left[B_v\right]^{T}\left[\psi_h\right]d\Omega$.
$\left[K_h\right]$	is the transmissivity matrix; $\left[K_h\right]=\int_{\Omega}\left[B_h\right]^{T}\left[\kappa\right]\left[B_h\right]d\Omega$.
$\left\{\Delta d\right\}$	is a vector of incremental nodal displacements.
$\left[B\right]$	is the strain-displacement matrix.
$\left[D\right]$	is the stress-strain matrix.
$\left\{\psi_h\right\}$	is the vector of nodal head shape functions.
$\left[B_v\right]$	is the volumetric strain-displacement matrix.
$\left[B_h\right]$	is the hydraulic gradient-nodal head matrix.
$\left[\kappa\right]$	is the permeability matrix.
$\left\{\gamma_w h\right\}$	is a vector of nodal total pore water head multiplied by the unit weight of the pore fluid.
Δt	is the time increment.

The first row of Equation 3.6 relates the change in internal forces (i.e. forces due to effective stress and pore water pressure) to the change in external forces during an increment of time, Δt. The stiffness matrix, $\left[K\right]$, relates the displacements at nodes to forces at nodes. The stiffness matrix, $\left[K\right]$, is formed using the effective stress versus strain relationship of the soil skeleton. Therefore, $\left[K\right]\left\{\Delta d\right\}$ represents the forces due to changes in effective stress. The transpose of the coupling matrix, $\left[K_v\right]$, relates pore pressures at nodes to forces at nodes. The difference in $\left.\left\{\gamma_w h\right\}\right|_{t+\Delta t}$ and $\left.\left\{\gamma_w h\right\}\right|_{t}$ is equivalent to the change in pore water pressure during Δt. Therefore, the difference between $\left.\left[K_v\right]^{T}\left\{\gamma_w h\right\}\right|_{t}$ and $\left.\left[K_v\right]^{T}\left\{\gamma_w h\right\}\right|_{t+\Delta t}$ represents the forces due to changes in pore pressure.

The second row of Equation 3.6 represents the seepage equation. The generalized trapezoidal finite difference method is used to discretize the transient seepage equation in the domain of time. If the variable, θ, is equal to one, the time marching scheme is fully implicit and unconditionally stable. Numerical method or finite element textbooks may be referenced for further details about the generalized trapezoidal finite difference method.

3.3. IMPLEMENTATION IN SAGE

Morrison (1995) describes the original development of the finite element program SAGE. SAGE was developed to be a useful and flexible tool for the analysis of static geotechnical engineering problems. The original version of SAGE solved static equilibrium problems governed by the partial differential equation:

$$\sigma_{ij,j} = 0 \qquad \text{Equation 3.7}$$

The original version of SAGE used the finite element formulation:

$$[K]\{\Delta d\} = \{\Delta F\} \qquad \text{Equation 3.8}$$

The stiffness matrix, [K], in Equation 3.8 is the same as in Equation 3.6. In the original version of SAGE, the stiffness matrix, [K], could be assembled using a stress-strain matrix relating effective stress to strain, or total stress to strain. Therefore, the original version of SAGE was suited to solving completely drained or completely undrained problems, but not problems where partial drainage (consolidation) takes place.

SAGE uses Newton-Raphson iteration for the solution of the finite element equations, which generally are nonlinear due to material non-linearity. SAGE was written in FORTRAN 77 using a structured programming style. The program is modular in the sense that each distinct programming task is contained in a subroutine. COMMON blocks are not used, and all information is passed between the main program and subroutines with argument lists.

The implementation of coupled consolidation into SAGE involved changes to pre-existing subroutines and the creation of new subroutines. Two goals guided the task of implementing coupled consolidation. The first was to preserve and build upon the modular structure of SAGE. The second was to add to SAGE's usefulness as a tool for analyzing geotechnical engineering problems. Appendix B contains a thorough description of the work involved in implementing coupled consolidation into SAGE.

3.4. VERIFICATION PROBLEMS

Three consolidation problems were analyzed with SAGE after implementing coupled consolidation within it. The results of these analyses were compared to analytical solutions of the same problems. The goal of analyzing these problems was to verify the correct implementation of coupled consolidation into SAGE.

TERZAGHI ONE-DIMENSIONAL CONSOLIDATION PROBLEM

The first verification problem analyzed was the consolidation of a column of soil restrained from lateral displacement. This is known as one-dimensional consolidation since the deformation and flow of pore fluid occur in only one direction. One-dimensional consolidation conditions apply when a layer of saturated clay of uniform thickness is subjected to a uniform surcharge, q, of large lateral extent. Terzaghi (1925) considered the problem of one-dimensional consolidation for the case of a surcharge applied instantaneously. Terzaghi made the following assumptions in his derivation of an analytical solution to the problem:

1. The soil is fully saturated with water.

2. The water in the pores of the soil is incompressible.
3. The soil skeleton is linear elastic.
4. The individual soil particles making up the soil skeleton are incompressible.
5. Darcy's Law governs the flow of the pore water through the soil skeleton.
6. The pore pressure increases by the amount of the surcharge when the surcharge is applied.

Terzaghi derived the following partial differential equation based on the assumptions listed above and the continuity of pore water flow:

$$c_v \frac{\partial^2 u}{\partial^2 z} = \frac{\partial u}{\partial t}$$ Equation 3.9

Where c_v is the coefficient of consolidation that is determined by the compressibility and permeability of the soil (length^2/time), u is the excess pore water pressure in the soil (force/ length^2), t is time, and z is depth (length).

Equation 3.9 can be solved using the separation of variables technique. Most textbooks on soil mechanics contain the solution to Equation 3.9.

Figure 3.1 illustrates the geometry, material properties, boundary and initial conditions of this problem. The finite element mesh shown in Figure 3.1 was used to model the problem. Ten 8-noded serendipity quadrilateral elements were used to model the soil column. Each of these elements has eight nodes for displacement and four nodes for pore water head. The application of the traction to the soil column cannot be modeled instantaneously, since time increments must be greater than zero to maintain the positive definiteness of the stiffness matrix. The traction was therefore modeled as a ramp loading over 0.5 days.

Figure 3.2 is a plot of the excess pore pressure with depth from the SAGE analysis and from Terzaghi's solution, at five different times. Time is represented by the time factor, T, which is a dimensionless number defined by $c_v t / H^2$. The excess pore pressure is normalized by the magnitude of the traction, q, and the

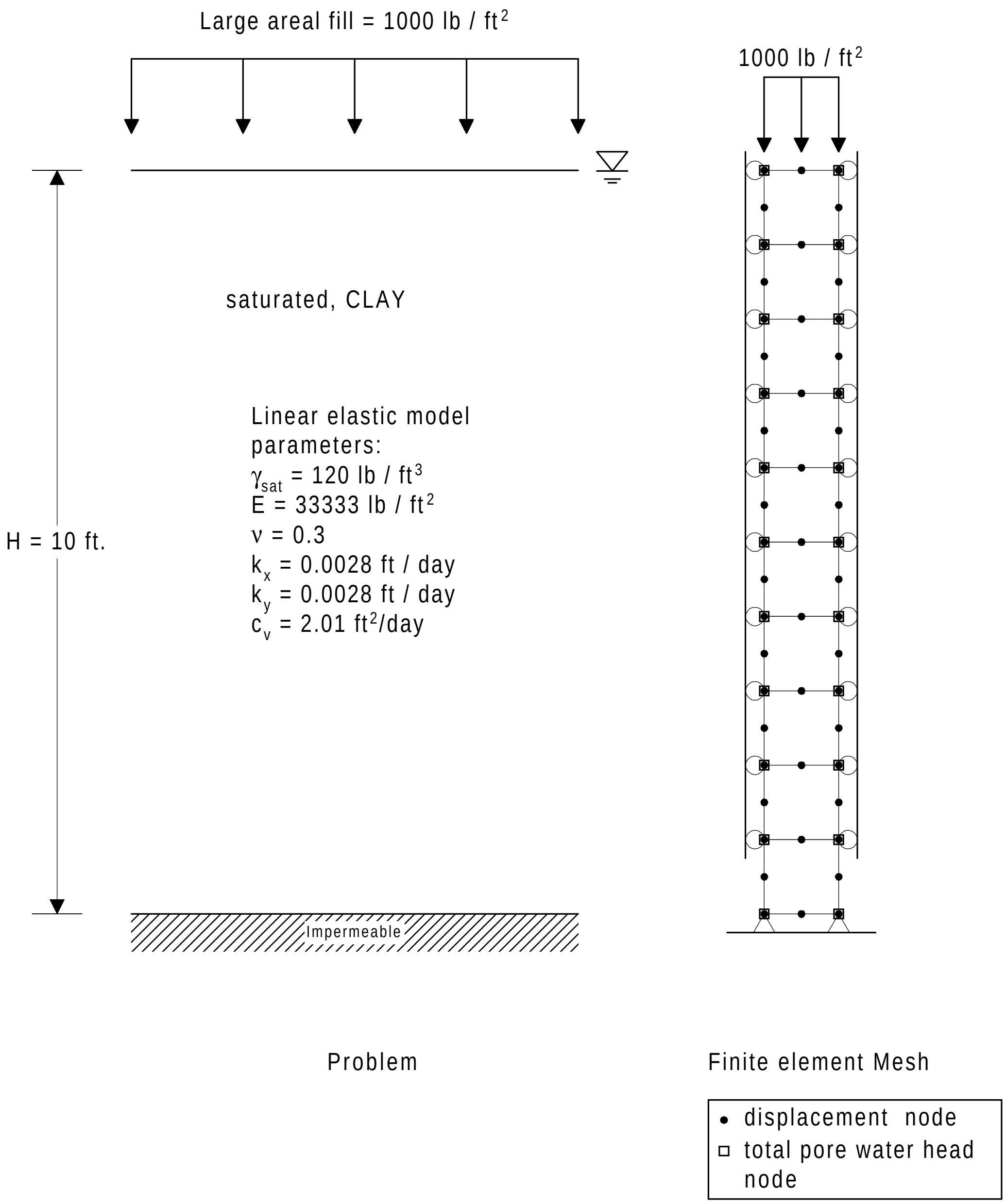

Figure 3.1. Geometry and finite element mesh for Verification Problem One.

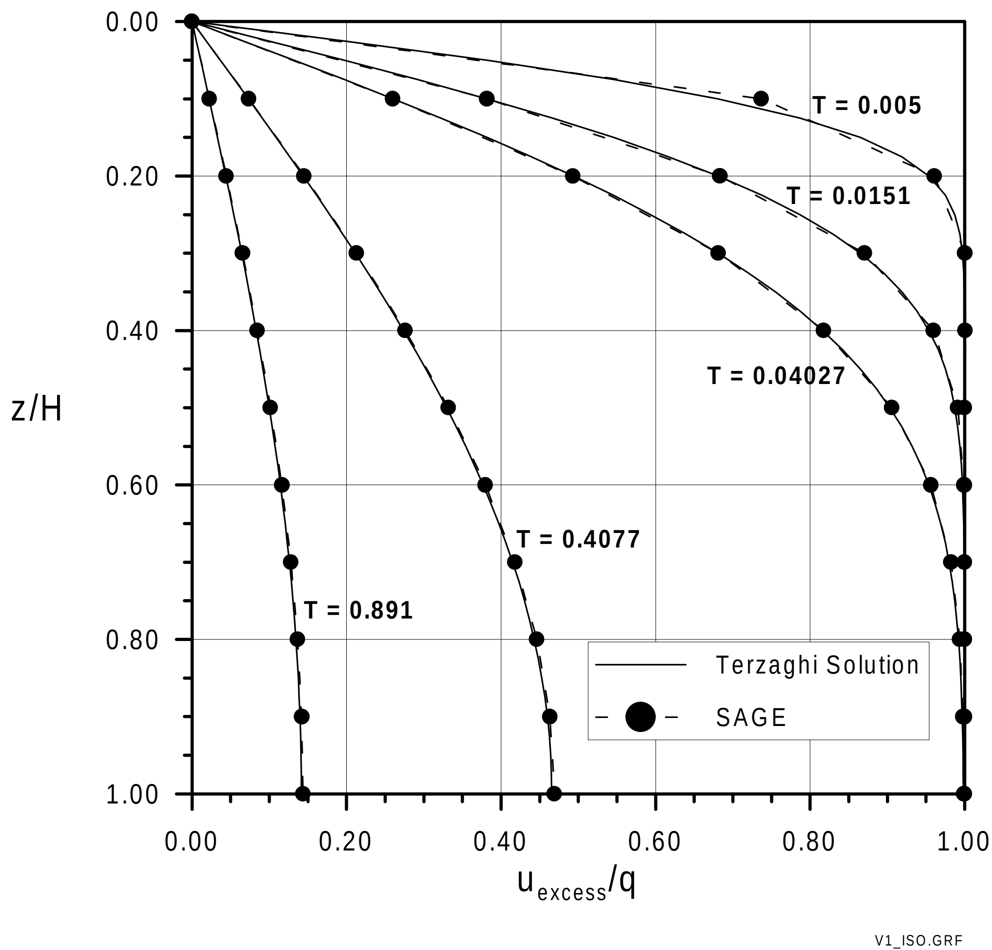

Figure 3.2. Pore pressure isochrones for Verification Problem One.

depth, z, is normalized by the length of the longest drainage path, H. The agreement between the results from SAGE and Terzaghi's solution is excellent.

There is a slight difference between the SAGE results and Terzaghi's solution at the very early stages of the problem. There are two causes of this difference. The first is the coarseness of the mesh. Since the pore pressure varies linearly over each element more elements of smaller size would be required in order to more closely approximate the true solution. The second is the manner in which the load is applied in the SAGE analysis. Terzaghi's solution assumes that the load is applied instantaneously at t = 0. This instantaneous load cannot be modeled in SAGE since time increments in a coupled analysis must be greater than zero. The load application was therefore modeled as a ramp loading over a small time interval. The ramp loading affects the results because consolidation takes place during the loading.

Figure 3.3 compares the average degree of consolidation from Terzaghi's theory and the results from SAGE. The degree of consolidation, U_z, is defined as $1-u/q$ at depth z. The average degree of consolidation is obtained by averaging U_z over the height of the soil column. Figure 2.3 shows that the agreement between SAGE and the theoretical solution is excellent.

ONE-DIMENSIONAL CONSOLIDATION OF TWO CONTIGUOUS LAYERS

The geometry, material properties, boundary conditions, and initial conditions for the second verification problem are shown in Figure 3.4. This problem involves two soil layers with different permeabilities make up the soil column. The permeability of the lower layer is one-fourth as great as the permeability of the upper layer. All other parameters are the same for both layers. Gray (1944) developed an analytical solution for the general case of one-dimensional consolidation of two contiguous layers of unlike compressibility and permeability

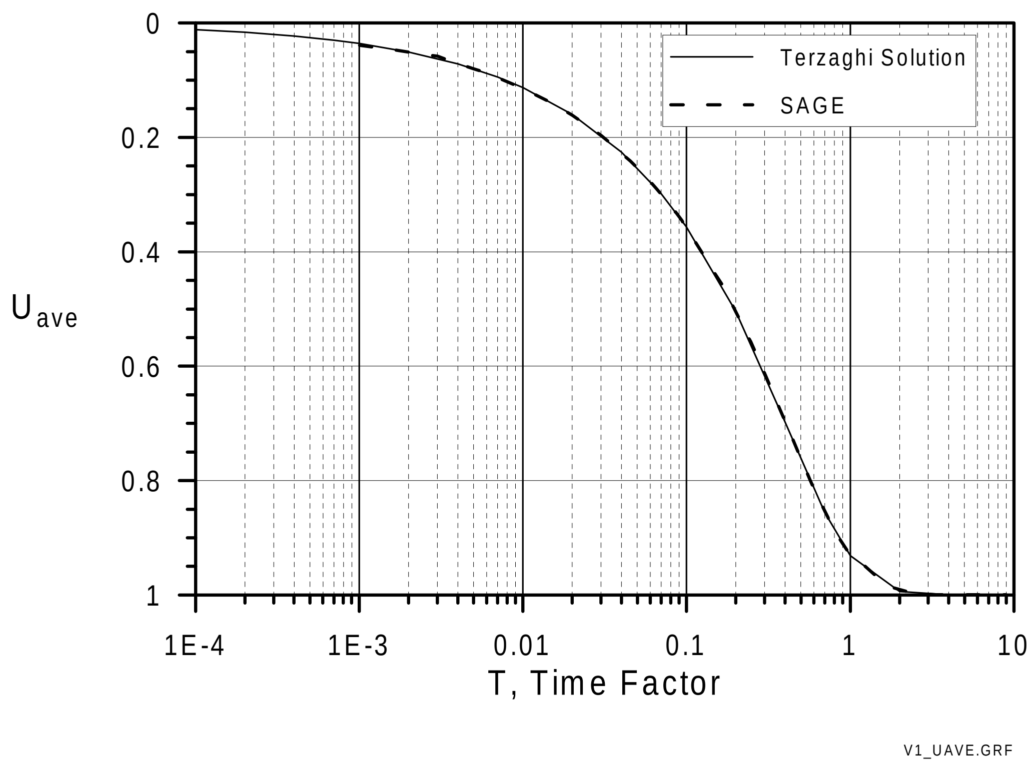

Figure 3.3. Degree of consolidation for Verification Problem One.

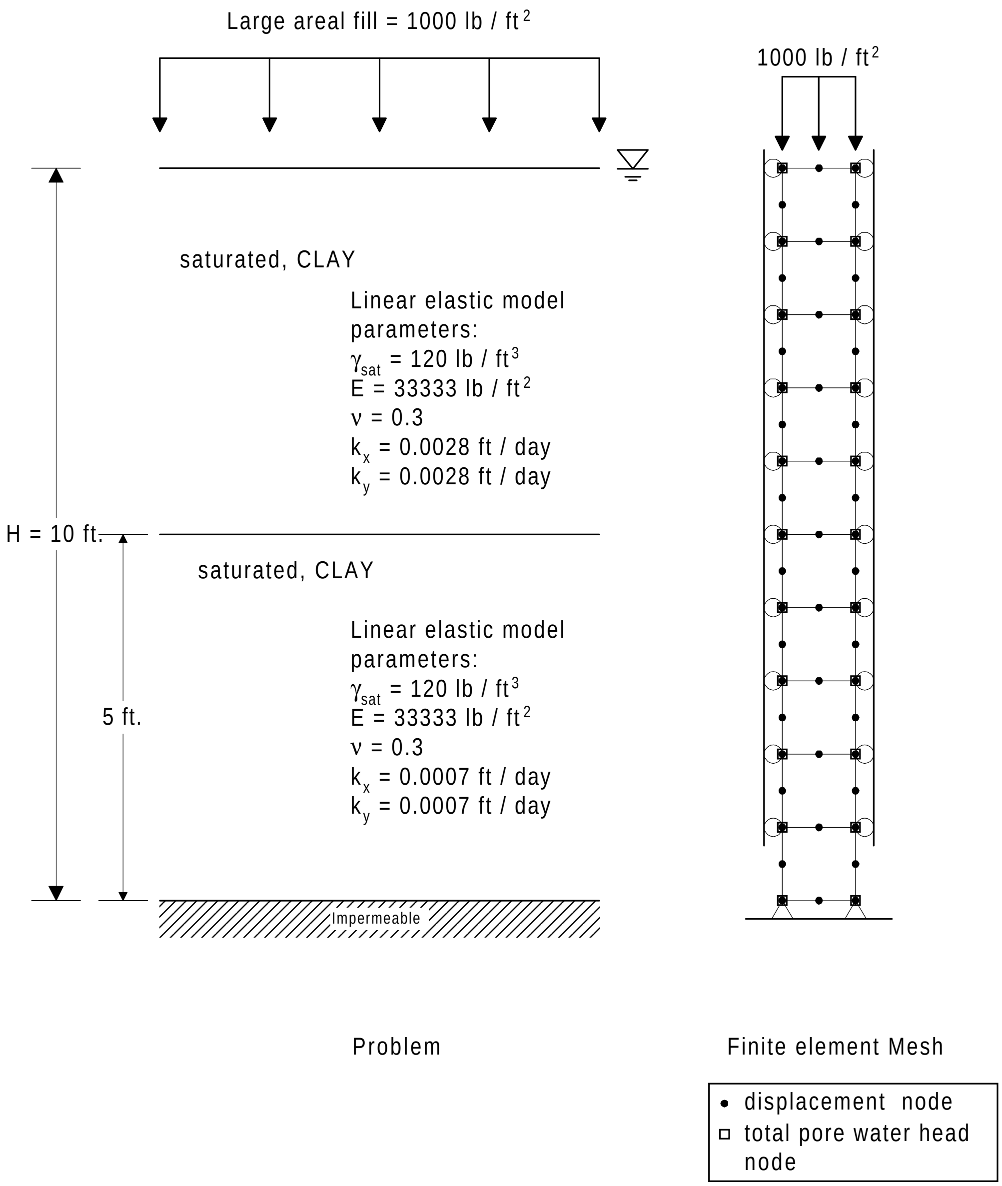

Figure 3.4. Geometry and finite element mesh for Verification Problem Two.

using the same assumptions that Terzaghi used. Gray's solution and its evaluation for this problem are presented in Appendix C.

Figure 3.5 compares normalized excess pore pressure versus depth from the SAGE results and Gray's solution. The agreement between the two solutions is very good. The ramp loading used in the SAGE analysis to model the instantaneous load application does cause a minor difference in the solution. Note that influence of the ramp loading decreases with time, since the consolidation process slows as it progresses.

Figure 3.6 is a plot of the average degree of consolidation from Gray's solution and from the SAGE results. The agreement between the two solutions is excellent.

STRIP FOOTING ON CLAY LAYER OF FINITE THICKNESS

The third verification problem is a two-dimensional consolidation problem involving a flexible strip footing on a clay layer of finite thickness. The clay layer is assumed to rest on a rigid impermeable base. The interface between the clay and the base is assumed to be perfectly smooth. The problem considered is shown in Figure 3.7. The soil is linear elastic and completely saturated with water. Gibson et al. (1970) derived an expression for the surface settlement of the clay layer using coupled consolidation theory. The Gibson et al. solution and the algorithm used in evaluating it for this problem are shown in Appendix C. The problem was analyzed with SAGE and compared to the Gibson solution for Poisson's ratio equal to 0.10 and 0.30.

Two finite element meshes were analyzed with SAGE for each value of Poisson's ratio. One mesh was a coarse mesh with 44 eight-noded quadrilateral elements and 163 nodes, and the second, finer mesh consisted of 176 eight-noded quadrilateral elements and 589 nodes. Both meshes are shown in Figure 3.8.

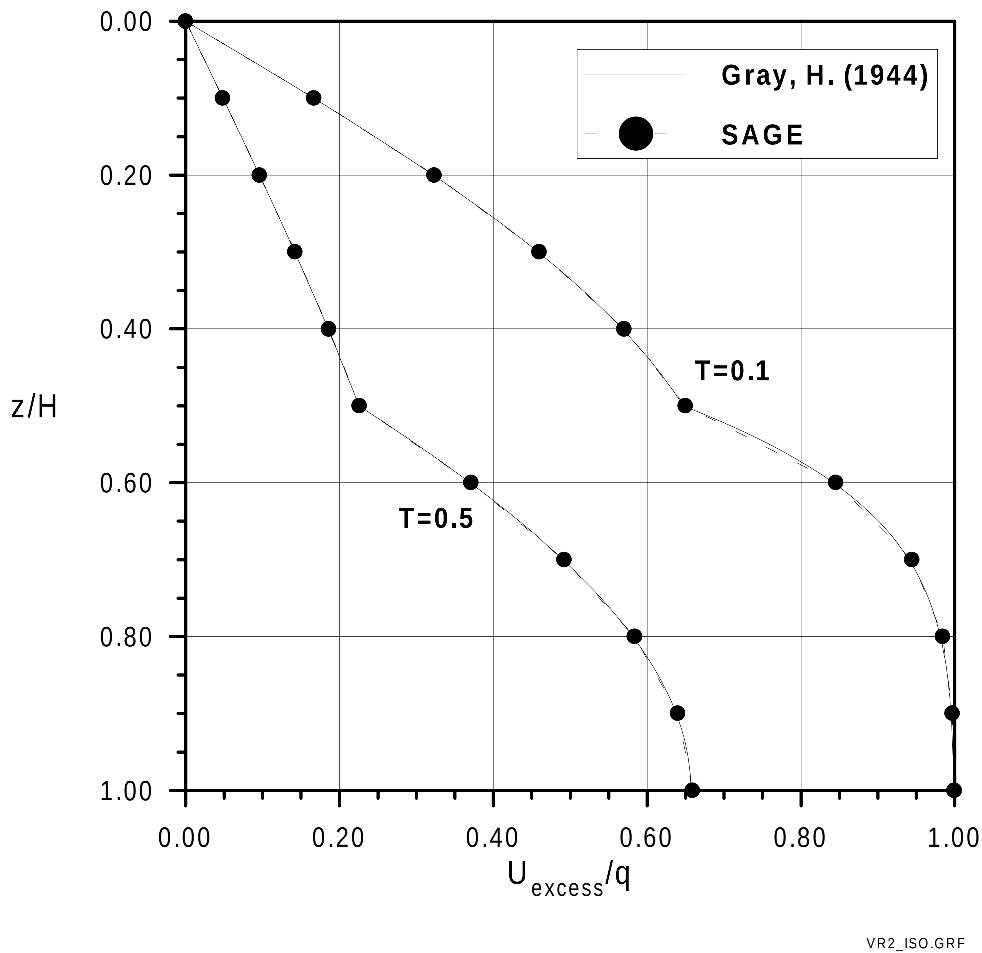

Figure 3.5. Pore pressure isochrones for Verification Problem Two.

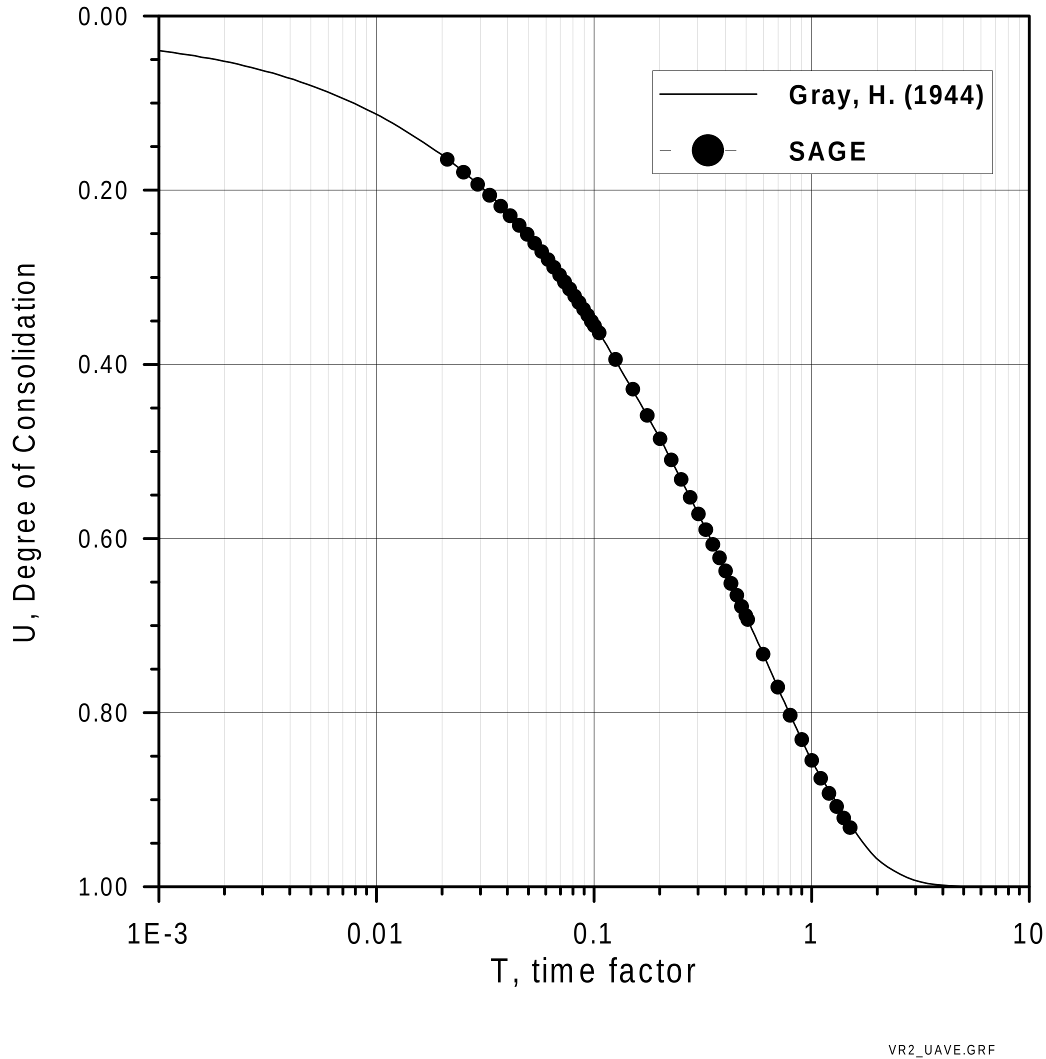

Figure 3.6. Degree of consolidation for Verification Problem Three.

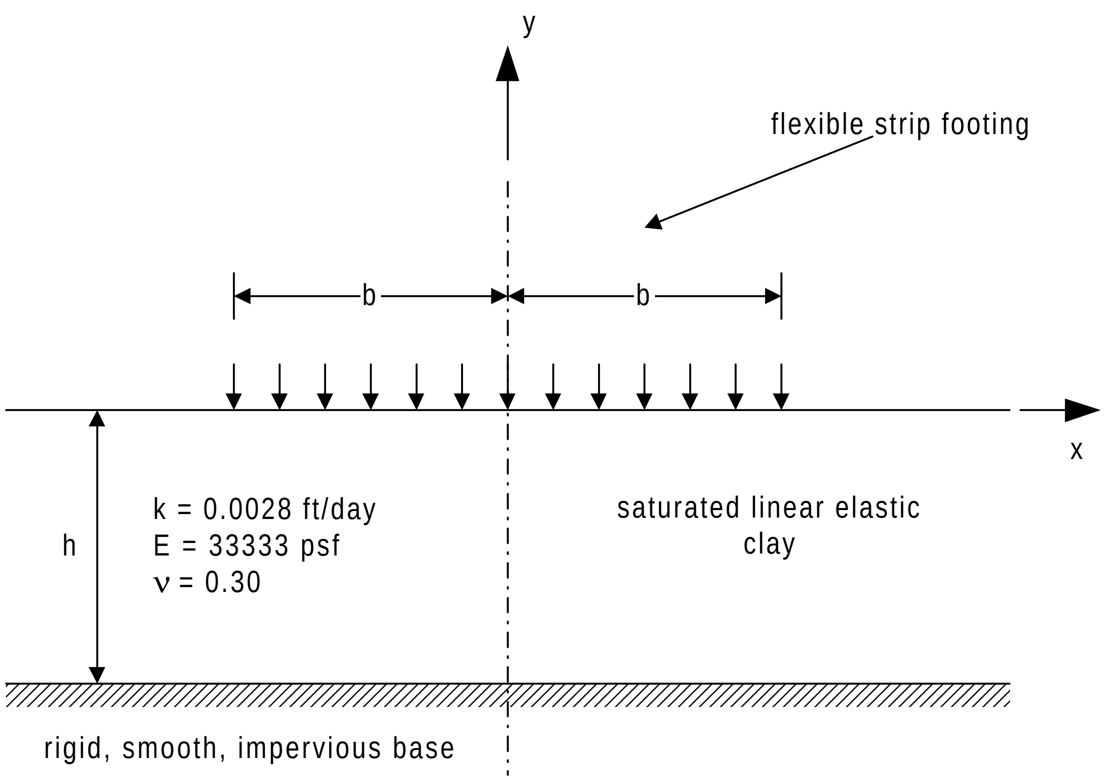

Figure 3.7. Verification Problem Three.

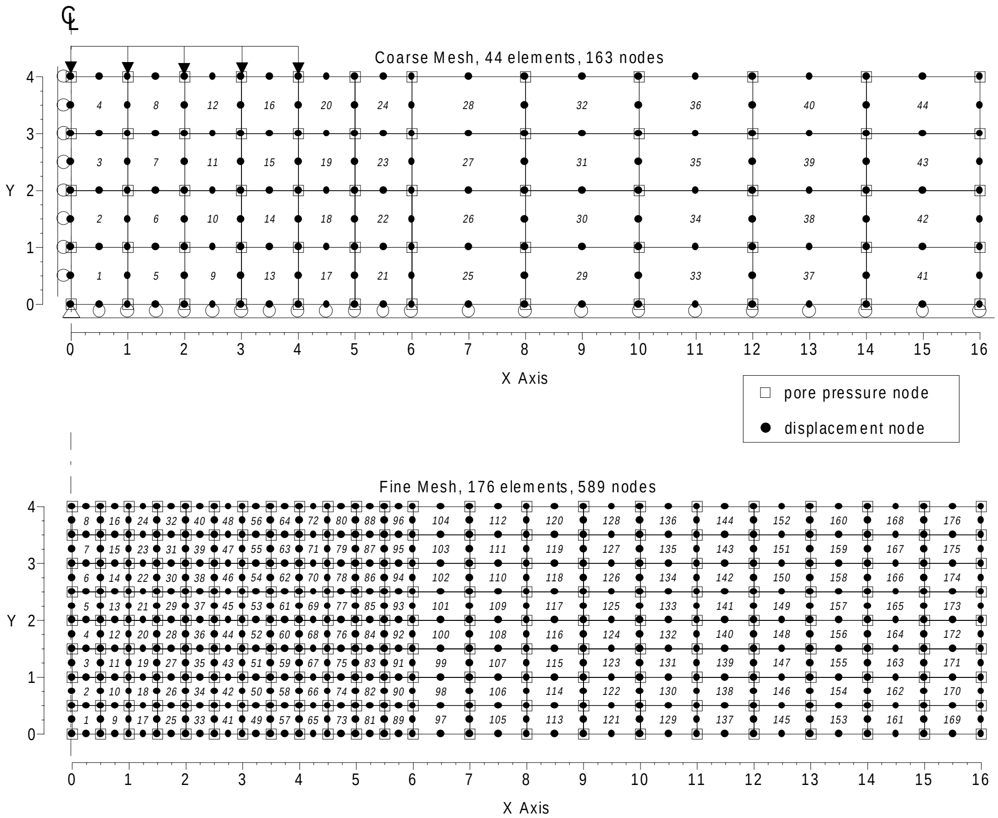

Figure 3.8. Finite element meshes for Verification Problem Three.

The strip load was applied as a ramp load applied during the first 0.05 days of the analysis. The Gibson et al. solution assumes that the loading is instantaneous. Figure 3.9 is a plot of normalized settlement at the centerline of the strip footing versus the time factor for the Gibson et al. solution and the SAGE results. The agreement between the two solutions is very good for both values of Poisson's ratio. The Gibson et al. solution and the SAGE settlements differ slightly at the very early stages of consolidation. The main cause of the difference is the discretization of the clay layer. Note that the difference between the SAGE results and the Gibson et al. solution is less for the fine mesh than for the coarse mesh. A second cause is that the strip loading is not instantaneous in the SAGE analysis, but it is instantaneous in the Gibson et al. solution.

Figure 3.10 is a profile of the normalized settlement of the surface of the clay layer at a time factor of 0.001 for the case of Poisson's ratio of the clay equal to 0.10. The agreement between the Gibson et al. solution and the SAGE results is very good. The settlement profile from the fine mesh agrees better with the analytical solution than the settlement profile from the coarse mesh.

3.5. CONCLUSION

Coupled consolidation was implemented into the finite element program SAGE. The implementation of coupled consolidation greatly expands the range of problems that SAGE can analyze. Three verification problems were analyzed with the new version of SAGE. The agreement between the SAGE results and analytical solutions for the verification problems is very good.

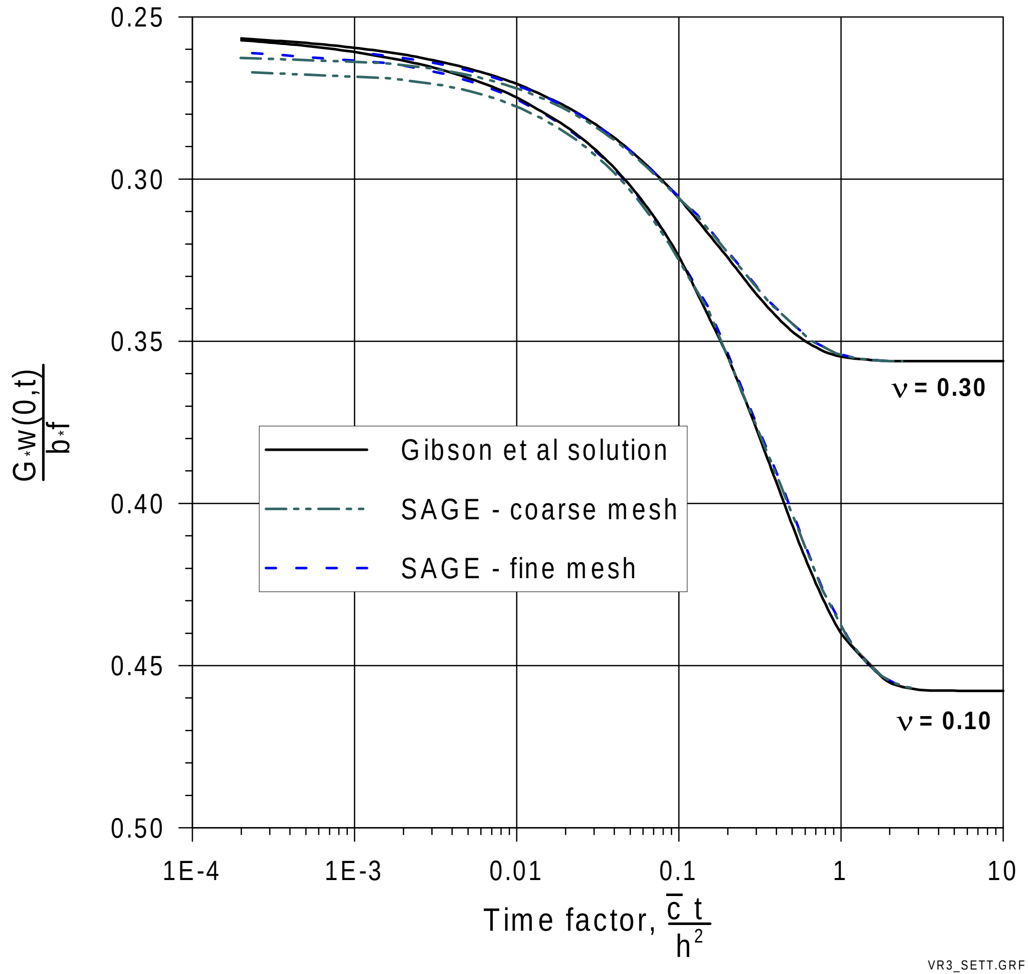

Figure 3.9. Normalized settlement versus time factor.

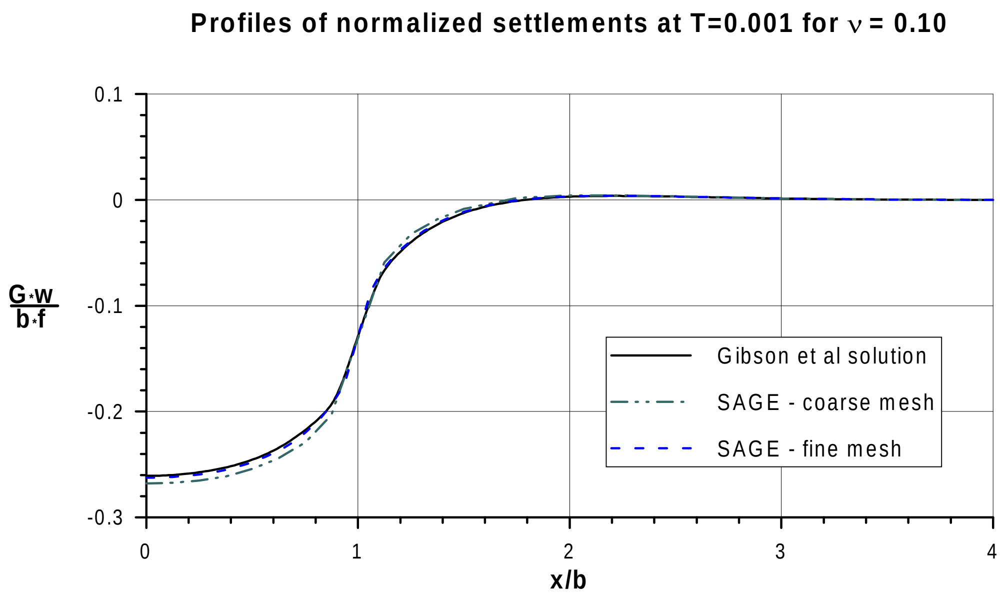

Figure 3.10. Normalized settlement profile of top of clay layer at T=0.001.